IEEE Access
Multidisciplinary | Rapid Review | Open Access Journal

Received February 6, 2020, accepted February 24, 2020, date of publication March 3, 2020, date of current version April 8, 2020.

Digital Object Identifier 10.1109/ACCESS.2020.2977985

Framework for Sizing of Energy Storage System Supplementing Photovoltaic Generation in Consideration of Battery Degradation

HUNYOUNG SHIN[1], (Member, IEEE), AND JAE HYUNG ROH[2], (Member, IEEE)
[1]Department of Electrical Engineering, Sangmyung University, Seoul 03016, South Korea
[2]Department of Electrical Engineering, Konkuk University, Seoul 05029, South Korea

Corresponding author: Jae Hyung Roh (jhroh@konkuk.ac.kr)

ABSTRACT There is growing interest in the use of energy storage systems (ESS) to create combined ''renewable energy plus storage'' power plants. ESS based on lithium-ion batteries have drawn much attention due to their high energy density and low self-discharge. However, as lithium-ion batteries are still costly, a power producer should determine ESS capacity in a sophisticated manner to ensure profitability of the PV plus storage projects. During the project horizon, lithium-ion batteries undergo severe capacity degradation, which must be considered in ESS planning. The degradation rate depends on various stress factors which are affected by ESS sizes and operation. Therefore, this paper aims to propose an advanced framework for calculating the capacity of an ESS supplementing a photovoltaic system considering the effect of the size and operation of ESS on battery degradation while maximizing profitability. Depending on how batteries are used during the project horizon, two scenarios are discussed and an ESS sizing framework for each scenario is suggested. To deal with non-convexity and black-box parameters of the optimal ESS sizing problems, we introduce an iterative algorithm that finds a solution by accessing battery degradation and optimizing profitability repetitively. We adopted the South Korean market for analysis and simulation of the frameworks.

INDEX TERMS Battery degradation, energy storage system (ESS), ESS sizing, economic analysis.

I. INTRODUCTION

The depletion of fossil fuel sources and continued threat of global warming have led to the emphasis of the importance of renewable energy development. As such, many governments around the world are attempting to expand renewable energy supply through financial incentives and regulatory policies. The Renewable Portfolio Standard (RPS), which has been widely adopted in the United States, the United Kingdom, China, and South Korea, is a regulation for renewable energy expansion that requires electricity providers to produce a percentage of electricity using renewable energy sources such as wind, solar, geothermal, and biomass. Some countries like the United States and South Korea also have renewable energy certificates (REC) programs. Generally, one REC is issued for each MWh of electricity generated and delivered to the grid using renewable energy. REC markets exist where energy supply companies trade RECs to meet RPS program obligations.

Solar energy has been adopted as one of the most important renewable energy sources because of its abundance and scalability, easily going from a few kWs to hundreds of MWs. Additionally, continued solar panel price decreases have led to rapid growth in solar installations. According to Lazard [1], the levelized cost of energy of solar in 2018 was lower than that of some conventional generation sources such as gas, nuclear, and, coal. However, because solar generation is intermittent and generally non-dispatchable, the solar generation's high penetration significantly affects power system operation. Some governments have started to focus on energy storage system (ESS) as a method for relieving such effects and established policies for promoting ESS installation in the countries. For example, California adopted an ESS procurement mandate of 1,325MW that applies to its three largest investor-owned utilities. The South Korean government grants additional REC weights to electricity discharged from ESSs

The associate editor coordinating the review of this manuscript and approving it for publication was Padmanabh Thakur.

that were charged using renewables to improve the profitability of ESS investors.

Among the various types of energy storage, lithium-ion batteries are used in electric vehicles because of their high energy density, light weight, low self-discharge rate, and long life span [2], [3]. Rapid electric vehicle proliferation has accelerated lithium-ion battery price decreases through economies of scale, and lithium-ion batteries are now economically viable to be used in power systems in some countries. Nevertheless, their prices remain high compared to other power generation sources. Therefore, ESS-based power producers should be very thoughtful in determining proper ESS sizes for securing profitability in their energy projects. Renewable energy projects including a PV plus storage typically last 10 to 20 years. During this period, batteries undergo significant degradation; therefore, degradation must be considered when determining ESS size. Battery degradation is affected by stress factors such as state of charge (SoC), depth of discharge (DoD), temperature, and C-rate, which are determined by ESS operating algorithms and battery specifications. ESS size is one of those specifications affecting such stress factors. In other words, different ESS sizes produce different stress factors, resulting in different battery degradation. Therefore, ESS size is a variable that affects battery degradation, which means the degradation rate is not an independent parameter of ESS sizes. Consequently, effective ESS sizing must take into account how battery degradation is affected by ESS sizes.

To analyze battery degradation, chemical theory [4]–[6] as well as empirical [7] and semi-empirical approaches [8]–[12] have been used. Analyzing battery degradation through chemical theory has the advantage of logically explaining degradation causes. However, data resulting from this approach are generally difficult to match with practical battery operation data. Empirical approaches can be another option, but such methods require large volumes experimental data to ensure accuracy. Empirical models based on limited data in one application typically cannot be applied to other applications. Semi-empirical approaches taken by references [8]–[12] combine theoretical analyses with empirical observations to model battery capacity degradation. Their models are flexible enough to be used for various energy storage applications while still showing a good fit with practical data.

In recent years, multiple studies have attempted to determine optimal energy storage planning in various applications. Some of these studies [13]–[17] have focused on ESS sizing and siting to improve power system flexibility as part of the system assets. Zhang et al. [18] and Qiu et al. [19] explored co-optimizing of transmission and storage planning. Energy storage planning for accommodating high renewable input in current power systems has been discussed in several studies [20]–[23], and other have focused on ESS sizing for power producers pursuing profit maximization [24]–[30]. These works disregard battery capacity degradation or treat it as an externally determined parameter which is independent of ESS size. However, degradation's relationship with ESS sizes shall be considered in calculating the optimal ESS capacity. Furthermore, in many of aforementioned works, ESSs are planned to take advantage of energy arbitrage from wholesale electricity markets. However, in practice, renewable energy is typically traded through long-term bilateral forward contracts or power purchase agreements (PPA) rather than on wholesale electricity markets to ease project financing and provide risk-hedging for energy projects. Power producers investing in renewable plus storage systems would also prefer to trade electricity through long-term forward contracts, but there is insufficient discussion on ESS sizing for this.

This paper presents an advanced ESS sizing framework based on an iterative method considering lithium-ion battery degradation. To the best of our knowledge, this is the first study that reflects the influence of ESS sizes and operation on battery degradation in proposition of an ESS sizing strategy. In this work, a brief discussion on the structures of PV plus storage systems is provided first. Next, we study battery degradation modeling, which is expressed as a complex function of stress factors based on Xu et al. [12]. We consider independent power producers who seek maximization of net present value (NPV) through a long-term contract or PPA. The rationale for this consideration is justified by the fact that in many countries renewable energy is commonly traded by long-term contracts or PPAs. Although this work focuses on the forward contract type which is typical for South Korea, the proposed framework can be applied to other markets or applications. From a practical perspective, we introduce two scenarios based on how to use batteries over the contract horizon and then formulate optimization problems for each scenario. However, these optimization problems are non-convex and highly nonlinear because battery capacity degradation depends on ESS sizes and operation in a very complicated sense. In fact, it is highly complex to express battery degradation as an analytic form of input variables in the optimization problems. To resolve these issues, we propose an iterative framework that repetitively applies an ESS operation algorithm, evaluates battery capacity degradation, and optimizes NPV at each iteration. From a simulation based on the South Korean forward contract type, we find that adding an ESS to an existing PV system is highly profitable. ESS sizes and profitability assessments are conducted by tuning forward contract prices and PV plus storage system parameters.

The main contributions of this work are enumerated below.

1) **Advanced ESS sizing framework considering interrelationship between ESS sizes and battery degradation:** This sizing strategy allows ESS investors to calculate more accurate ESS capacity than treating battery degradation as an independent parameter. The mathematical problems for optimal ESS sizing are not guaranteed to be convex and have black-box parameters. To resolve these issues, we propose an algorithm that evaluates battery degradation and optimizes economic values in an iterative manner.

2) **Different ESS sizing algorithms depending on battery usage types over the contract horizon in a practical perspective:** The first scenario assumes that a constant maximum battery capacity is used for the entire contract horizon. The second scenario fixes a maximum DoD range during the contract period. We suggest a ESS sizing strategy for each scenario.
3) **Various numerical experiments:** We calculate ESS sizes and economic values using the proposed framework with various system conditions such as PV system capacities, DC converter sizes, maximum DoD ranges, and PPA contract prices.

The rest of this paper is structured as follows. Section II describes PV plus storage systems and electricity markets. Section III models battery capacity degradation, Section IV presents the proposed frameworks, and Section V provides numerical results. Lastly, the paper is concluded in Section VI.

II. SYSTEM DESCRIPTION

A. PV PLUS STORAGE SYSTEM DESCRIPTION

Depending on the degree to which the storage and PV are physically and operationally coupled, a PV plus storage system can be categorized as either an AC-coupled or DC-coupled PV plus storage system [31], [32]. Figure 1 shows a schematic diagram of an AC-coupled system with co-located PV and ESS that share a point of common coupling with the AC power grid. The PV and ESS can operate independently in this system because they do not share any power electronic devices. Thus, the system operator is free to select between the grid and PV to obtain the electricity source that maximizes profits. Because of this flexibility, such a system cannot prove the origin of electricity charging the ESS. Therefore, this system type cannot receive financial incentives such as federal investment tax credits (ICT) in the United States and extra REC weights in South Korea. Figure 2 presents a schematic diagram of a DC-coupled system in which the PV and ESS are coupled the on the DC side and share an AC-DC inverter. The ESS can store PV electricity through the DC-DC converter in this system, but it cannot be charged from the grid. Therefore, this system is eligible for ICT or extra REC weights, increasing the profitability for the system owner. In many markets, including North America, developers are increasingly interested in DC-coupled systems for this reason [33]. The remainder of this paper assumes DC coupled systems as shown in Figure 2.[1]

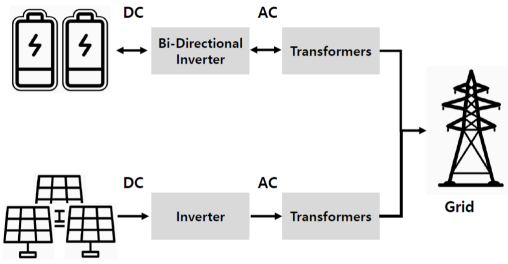

FIGURE 1. Schematic diagram of an AC-coupled system.

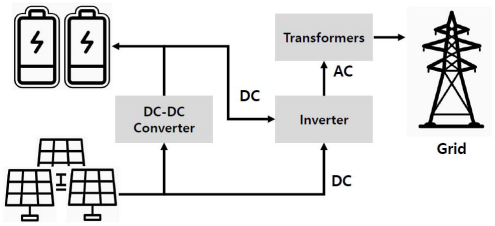

FIGURE 2. Schematic diagram of a DC-coupled system.

B. ELECTRICITY MARKET DESCRIPTION

Solar energy is commonly sold through long-term forward contracts in which a power supplier and purchaser agree on an electricity price for a fixed period that typically ranges from 10 to 20 years. However, there have been some discussions on participating in wholesale electricity markets [34]–[36]. On the one hand, solar power producers can guarantee a long-term steady source of revenue through forward contracts, which allows them to facilitate project financing. On the other hand, buyers, typically a utility or large corporation, can be supplied low price power and attain RECs to meet the RPS. Recently, growing number of PV plus storage projects ranging from few MWs to tens of MWs have come online in the United States. Because a PV plus storage system has much greater flexibility in supplying power, a project owner would expect to sign a higher-price contract than with a standalone PV system. The rough forward contract price ranges of some PV plus storage projects are accessible; however, sensitive information about PPA contracts such as ESS operating conditions and the detailed structure of contract prices are not published. Unlike in the United States where many utilities exist, South Korea has only one utility company known as Korea Electric Power Corporation (KEPCO). Power generated from renewables and RECs are both tradable either through spot markets or bilateral contracts with KEPCO.

Table 1 shows various solar power REC weights for different capacities and installation types. In the case of PV plus storage, electricity discharged from the ESS that were produced by PV between 10:00 and 16:00 is eligible for 5.0 REC until the end of 2019 and 4.0 REC in 2020. For PV-generated power directly supplied to the grid, REC weights between 0.7 and 1.5 are imposed. Unlike traditional power generation companies, renewable power providers are exposed to both volatile system marginal prices[2] and REC prices, which makes it difficult for renewable energy providers to expect stable profits and thus makes providers reluctant to invest in renewable energy. To ease of this uncertainty, the South Korean government have approved a long-term forward contract and introduced so-called ''fixed price markets'' where

[1]There are the other designs of DC-coupled system types besides the one shown in Figure 2.

[2]In South Korea, system marginal price or SMP which is the shadow price of the system balance constraint determines wholesale electricity prices.

TABLE 1. REC weights for PV systems based on installation types and sizes in South Korea.

Install. Types	Sizes	REC Weights
On Land	$<$ 100kW	1.2
	$\geq$ 100kW	1.0
	$\geq$ 3000kW	0.7
On Building	$\leq$ 3000kW	1.5
	$>$ 3000kW	1.0
PV + Storage	-	5.0 (until 2019)
	-	4.0 (in 2020)

renewable energy providers can sell power and RECs to at long-term fixed prices. This is almost identical to ''bundled'' PPAs in the United States. In this paper, we consider the PV plus ESS system operator to be participating in fixed price markets or bundled PPAs.

III. LITHIUM-ION BATTERY DEGRADATION

Battery capacity degradation is a main concern for power providers as it directly affects profit. Batteries are chemical products, thus it is nearly impossible to analyze their degradation through a single method. This paper adopts a hybrid model combining chemical theory and the data-based model presented in Xu et al. [12].

Before discussing capacity degradation modeling, we must define battery capacity. Battery capacity is the energy (kWh) presently available in a battery. Thus, battery capacity decreases as the battery is used. In many academic works, battery life is defined as the time at which battery capacity reaches 80% of its initial capacity. However, in practice, lithium-ion battery manufacturers and ESS-based generation project developers sometimes adopt lower levels to calculate battery life.[3] Lithium battery degradation is divided into cycling aging caused by battery usage and calendar aging, which is naturally degradation over time. Total aging is the sum of these two types of aging. There are various stress factors that affect battery degradation such as DoD and SoC levels, C-rate, cycle numbers, temperature, and total battery operation time. Xu et al. [12] presented aging models for these factors based on a combination of chemical theory and experimental data analysis, which can be expressed as:

$$\text{DoD}: f_{DoD}(DoD) = (k_{DoD_1} DoD^{k_{DoD_2}} + k_{DoD_3})^{-1} \quad (1a)$$

$$\text{SoC}: f_{SoC}(SoC) = e^{k_{SoC}(SoC - SoC_{ref})} \quad (1b)$$

$$\text{C-rate}: f_C(C) = e^{k_C(C - C_{ref})} \quad (1c)$$

$$\text{Temp.}: f_T(T) = e^{k_T(T - T_{ref}) \cdot \frac{T_{ref}}{T}} \quad (1d)$$

where k_{DoD_1}, k_{DoD_2}, and k_{DoD_3} are DoD aging model coefficients and k_{SoC}, k_C, and k_T are SoC, C-rate, and temperature aging model coefficients, respectively. The subscript *ref* represents reference values for each stress factor ($SoC_{ref} = 50\%$, $C_{ref} = 1C$, and $T_{ref} = 25°C$). The number of cycles is calculated using the rainflow-counting algorithm [37] which is widely used in fatigue analysis. The mathematical model of battery capacity degradation can be given as the sum of cycling aging and calendar aging [12]:

$$f_d = \sum_{i=1}^{N} f_{DoD}(DoD_i) f_{SoC}(SoC_i) f_C(C_i) f_T(T_i) n_i + k_t H f_{SoC}(SoC_{avg}) f_T(T_{avg}) \quad (2)$$

where i represents the i-th cycle, H denotes total operation time in seconds, $SoC_{avg} = \sum_{i=1}^{N} SoC_i/N$, and $T_{avg} = \sum_{i=1}^{N} T_i/N$.

Because degradation is influenced by the battery's residual capacity and the solid electrolyte interphase phenomenon [38], battery state of health (SoH) can be modeled as follows:

$$SoH = p_{SEI} \cdot e^{-r_{SEI} f_d} + (1 - p_{SEI}) \cdot e^{-f_d} \quad (3)$$

Xu et al. [12] obtained a set of model parameters for Eqs. (2) and (3) from data on lithium-ion Manganese Oxide (LMO) battery degradation.

IV. ENERGY STORAGE SYSTEM SIZING FRAMEWORK

We must solve a problem with parameters dependent upon a decision variable in a highly complicated sense. That is, SoH considered in the optimization problem has a highly nonlinear relationship with battery size. Moreover, it is highly complex to express SoH as a mathematical function of ESS size as the stress factors determining SoH are affected by ESS operation. Therefore, this section's main focus is proposing an optimization strategy that deals with black-box parameters whose qualification is possible only through numerical computations. Before formulating the problem, we discuss two scenarios on how batteries are used during the project horizon or over the contract period. This is worth discussion because ESS project developers commonly require a minimum storage capacity or DoD range to be maintained during the project horizon or contract period, in practical situations. We assume that the contract period is sufficiently long-term to be the same as the project horizon.

A. SCENARIOS DEPENDING ON BATTERY USE

The first scenario assumes a constant usable capacity over the entire contract period, with the ESS operator using a fixed kWh range of the battery as shown in Figure 3(a). Because of capacity fade, the initial battery size should be considerably larger than usable energy. In this scenario, the goal is to determine the optimal usable energy and the degree of oversizing that maximizes the economic value of adding the ESS to an existing PV system. We refer to this scenario as ''Energy-Fix'' throughout the paper.

The second scenario assumes a constant % range or DoD used over the contract horizon. The usable capacity is calculated as the product of DoD and total capacity subject to degradation. That means that in this scenario, referred to as ''DoD-Fix'', the usable capacity decreases over time as

[3]This is because PPA between a power producer and utility is typically long-term, from 10 to 20 years. To meet end-of-life (EOL) set to 80%, ESS should maintain a maximum DoD range and C-rate at low levels to reduce battery degradation. It probably leads to low NPVs.

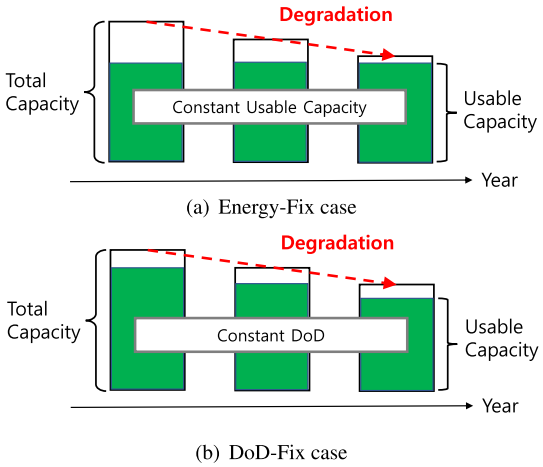

FIGURE 3. Total capacity and usable capacity of the battery in two scenarios.

shown in Figure 3. The goal then is to optimize ESS size with a predefined DoD value.

There could be additional scenarios, such as the combination of those two scenarios in such a way that usable capacity is fixed for the first half of the period and DoD is fixed for the other half.

B. ESS OPERATION ALGORITHM

The ESS operation algorithm for maximizing profits under South Korean type PPAs is not complex. Based on the REC weights listed in Table 1, storing as much PV generation from 10:00 to 16:00 as far as ESS capacity will allow is optimal. At other times, directly supply PV power to the grid is optimal because of round-trip battery losses. Thus, the optimal ESS operation strategy is described as follows:

(1) From 10:00 to 16:00 (6 hours):
   a. Store PV-generated power until the maximum SoC level is reached
   b. Supply remaining PV power directly to the grid

(2) Other times (18 hours):
   a. Supply PV-generated power directly to the grid
   b. Discharge electricity from the ESS at a constant rate until the minimum SoC level is reached

Remaining PV power in (1)-b involves power that cannot be stored in the ESS due to the limits of the battery and converter capacities in (1)-a. It should be noted that the maximum SoC level in (1)-a is constant in DoD-Fix as a fixed DoD range is used over the project horizon. In Energy-Fix, however, the level increases with time as described in Figure 3(b).

C. BATTERY SIZING STRATEGY CONSIDERING CAPACITY DEGRADATION

We start by formulating each scenario's optimization problem. Table 2 gives variables and parameters to be used in problem formulation. Because an ESS has one cycle every day, we do not need to solve the problem over an hourly basis but rather daily, which remarkably reduces problem formulation and computation complexity. Daily PV power production ($\tilde{G}_{PV}$) is set to a random variable to capture uncertainty. α_t is parameterized by year t because of PV panel degradation. Strictly speaking, α_t is random, but its variation is normally smaller than that of $\tilde{G}_{PV}$. Thus, we treat α_t as a scalar to avoid complexity caused by introducing two random variables in the problem solving process. For the South Korean market, λ_{ESS} becomes SMP+Weight×REC and λ_{PV} becomes SMP+1.0×REC.[4] C_{ESS} is the capital cost of a fully installed ESS including battery racks, system balancers, energy management systems, developer margins, and engineering, procurement, and construction costs, on a \$/kWh basis, excluding the DC converter. We assume that the existing PV system is equipped with a sufficiently sized AC-DC inverter.

1) ESS SIZING FOR ENERGY-FIX

Because long-term investment is of interest, it is necessary to consider the discounted value of cash flow to measure profitability. We employ NPV for the measurement. The ESS installation problem's NPV can be expressed as

$$\mathrm{NPV}(x, y) = \sum_{t=1}^{T} \gamma^t N \cdot \mathbb{E}[\mathrm{Rev}_t(x)] - C_{ESS} \cdot (1 + y)x \quad (4)$$

where $\mathbb{E}[\cdot]$ is the expectation over $\tilde{G}_{PV}$ and $\mathrm{Rev}_t(x)$ stands for revenue attained from ESS operation for each cycle in year t. DC converter size is assumed to be fixed, so it is not considered in Eq. (4). The influence of DC converter size will be discussed in sensitivity analysis by simulation. Before presenting how $\mathrm{Rev}(x, y)$ is formed, we define energy that can be stored in the ESS which is determined by ESS capacity and PV generation during 10:00-16:00 as

$$E_t(x) = \min\{Rx,\ \rho_{PV-Bat} \cdot \alpha_t k^t \cdot \tilde{G}_{PV}\}. \quad (5)$$

Although we consider the fixed energy case, DoD range R can also be included in (5) if DoD value is required. Now the revenue is

$$\mathrm{Rev}_t(x) = \lambda_{ESS} \cdot \rho_{Bat-AC} \cdot E_t(x) + \lambda_{PV} \cdot \rho_{PV-AC} \left(k^t \tilde{G}_{PV} - \frac{E(x)}{\rho_{PV-Bat}} \right) \quad (6)$$

with the first term representing revenues from ESS discharge and the second term representing revenues from directly supplying of PV-generated power to the grid.

Because usable capacity must be guaranteed for every $t \in T$, the problem requires the following conditions:

$$(1 + y) \cdot SoH_t(x, y) \geq 1 \quad \text{for } t = 1, \ldots, T. \quad (7)$$

[4]Of course, REC weights from 0.7 to 1.2 are imposed on a standalone PV system relying on its location and size as shown in Table 1. This work assumes a REC weight of 1.0 for such a system.

TABLE 2. Variables and parameters used for problem formulation.

x	Usable energy of ESS which a decision variable (in kWh)
y	Oversizing ratio which is a decision variable (scalar)
z	Energy capacity of ESS which a decision variable (in kWh)
λ_{ESS}	Forward contract price for electricity discharged from ESS (in \$ per kW)
λ_{PV}	Forward contract price for electricity from PV generation (in \$ per kW)
$\tilde{G}_{PV}$	Daily PV generation which is random (in kWh)
C_{ESS}	ESS system price (in \$ per kWh)
ρ_{Bat-AC}	Efficiency factor from the battery to the AC grid (scalar)
ρ_{PV-Bat}	Efficiency factor from the PV system to the battery (scalar)
ρ_{PV-AC}	Efficiency factor from the PV system to the AC grid (scalar)
R	Depth of Discharge (DoD) Range (scalar)
α_t	Ratio of PV generation during 10:00-16:00 to daily PV generation at year t (scalar)
T	The period of the contract or the ESS project (in years)
γ	Discount factor based on the discount rate r (scalar)
N	Number of charge and discharge cycles per year (scalar)
k	Degradation factor for the PV generation (scalar)

We can disregard $(1+y)\cdot SoH_t(x,y) \geq 1,\ \forall t = 1,\ldots,T-1$ because $SoH_t(x,y)$ does not increase with t. Thus, the optimization problem can be expressed as

$$\max_{x,y}\ \text{NPV}(x,y) \text{ in } (4) \tag{8a}$$

$$\text{s.t. } (1+y)\cdot SoH_T(x,y) \geq 1. \tag{8b}$$

The problem (8a)-(8b) is difficult to solve because of the bi-linear term in the objective function. Furthermore, we do not know the analytic form of SoH in the constraint whose qualification is only possible through computation.[5] To find the x and y values close to optimal, we decompose the problem and apply an iterative method. With a fixed $y = \hat{y}$, maximizing NPV$(x,\hat{y})$ becomes a convex problem with x which is analytically solvable. The first order condition for maximizing NPV$(x,\hat{y})$ is given by

$$\sum_{t=1}^{T}\gamma^t N\left(\lambda_{ESS}\rho_{Bat-AC} - \lambda_{PV}\frac{\rho_{PV-AC}}{\rho_{Bat-AC}}\right) \times\left[1 - F_{\tilde{G}_{PV}}\left(\frac{Rx^*}{\alpha_t k^t \rho_{Bat-AC}}\right)\right] = \frac{C_{ESS}(1+\hat{y})}{R} \tag{9}$$

where $F_{\tilde{G}_{PV}}$ denotes the cumulative distribution function of $\tilde{G}_{PV}$. The process for deriving Eq. (9) is provided in VI-A. Thus, we can easily find a value of x that maximizes NPV whenever y is fixed.

The proposed framework to find the storage size for Energy-Fix is as follows:

1) Initialize oversizing level y (e.g., $y = 0.3$).
2) For the given value of y, solve Eq. (9) to find the value of x that optimizes NPV.
3) With ESS capacity $(1+y)x$, apply the ESS operation algorithm given in Section IV-B and calculate stress factors to battery degradation. From Eq. (3), calculate SoH at the end year of the contract period, $SoH_T(x,y)$.
4) For a small positive number ϵ,
   (a) If $|(1+y)\cdot SoH_T(x,y) - 1| \leq \epsilon$, set the ESS size to x.
   (b1) If $(1+y)\cdot SoH_T(x,y) - 1 > \epsilon$, decrease y.
   (b2) If $1 - (1+y)\cdot SoH_T(x,y) > \epsilon$, increase y.
   After updating y, go back to step 2.

There are multiple ways to update y; however, we adopted a bisection method that repeatedly bisects the interval of y. The proposed framework assumes an arbitrary oversizing level and calculates optimal ESS size using a given oversizing level. It then checks whether the SoH constraint in Eq. (8b) is satisfied. If SoH at T has a positive slack greater than ϵ, we decrease the oversizing level under the assumption that the ESS was oversized. In the opposite case, we increase the oversizing level, assuming the ESS was undersized. Figure 4 illustrates the flow of this framework. The framework calls for one SoH evaluation that requires demanding computations at one iteration. Hence, the proposed framework is computationally efficient. To further reduce the computational burden, a suboptimal solution to Eq. (9) with an analytical form, which is described in VI-B, can be used in the second step.

2) ESS SIZING FOR DOD-FIX

In this scenario, the ESS operator uses the battery while fixing a DoD level thus reducing usable energy with battery degradation. Thus, energy to be stored in the ESS is limited by the degraded battery capacity, which can be expressed as follows:

$$E_t(x) = \min\left\{SoH_t(x)\cdot Rx,\ \rho_{PV-Bat}\cdot\alpha_t k^t \tilde{G}_{PV}\right\}. \tag{10}$$

[5]There might be an approximate analytic model but this requires large practical data, which is not yet plausible in the ESS-based generation industry.

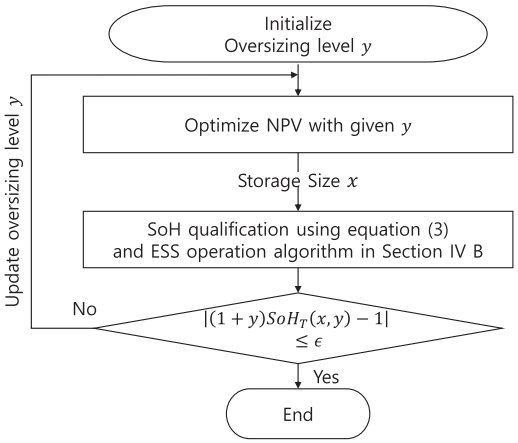

FIGURE 4. The ESS sizing framework considering battery degradation for Energy-Fix case.

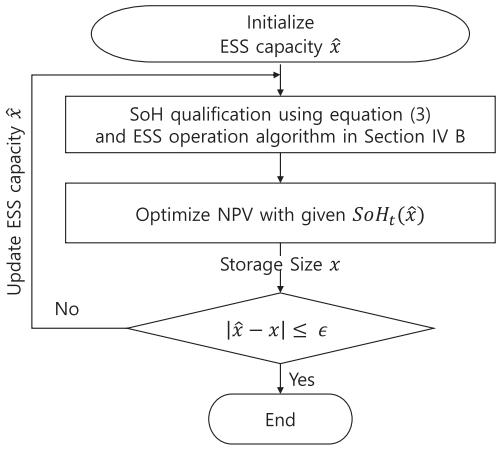

FIGURE 5. The ESS sizing framework considering battery degradation for DoD-Fix case.

The revenue equation has the same form as Eq. (6) except that now $E_t(x)$ changes from Eq. (5) to Eq. (10). Oversizing is not considered, thus the form of NPV is slightly altered from Eq. (4) to

$$\text{NPV}(x) = \sum_{t=1}^{T} \gamma^t N \cdot \mathbb{E}[\text{Rev}_t(x)] - C_{ESS} \cdot x. \tag{11}$$

We do not consider SoH constraints in the DoD-Fix case in this paper. Consequently, the optimization problem can be expressed as

$$\max_{x} \ \text{NPV}(x) \text{ in (11)}. \tag{12}$$

This problem is difficult to solve because of the product term, $SoH_t(x) \cdot Rx$. As with Energy-Fix, it would be effective to find a suboptimal solution to problem (12) by adopting an iterative method. If $SoH_t(x)$ is assumed to be scalar, problem (12) becomes a convex problem, which can be solved analytically. By fixing $SoH(x) = SoH(\hat{x})$ and using a similar process in VI-A, we can obtain the following condition for the optimal solution, x^*, to problem (12) under the condition $SoH(x) = SoH(\hat{x})$:

$$\sum_{t=1}^{T} \gamma^t N \cdot SoH_t(\hat{x}) \left(\lambda_{ESS} \rho_{Bat-AC} - \lambda_{PV} \frac{\rho_{PV-AC}}{\rho_{Bat-AC}} \right) \times \left[1 - F_{\tilde{G}_{PV}} \left(\frac{SoH_t(\hat{x}) R x^*}{\alpha_t k^t \rho_{Bat-AC}} \right) \right] = \frac{C_{ESS}}{R}. \tag{13}$$

The proposed framework for calculating the storage size for DoD-Fix consists of:

1) Initialize ESS capacity $\hat{x}$.
2) With $\hat{x}$, apply the ESS operation algorithm from Section IV-B and obtain battery degradation stress factors. Then calculate $SoH_t(\hat{x})$ for $t = 1, \ldots, T$ using Eq. (3).
3) Using $SoH_t(\hat{x})$ for $t = 1, \ldots, T$, find the value of x that solves Eq. (13).
4) For a small positive number ϵ,
   (a) If $|\hat{x} - x| \leq \epsilon$, set the ESS size to x.
   (b1) If $\hat{x} - x > \epsilon$, decrease $\hat{x}$.
   (b2) If $x - \hat{x} > \epsilon$, increase $\hat{x}$.

   After updating $\hat{x}$, go back to step 2.

The bisection method is employed to update $\hat{x}$. The framework first regards SoH at the current iteration as $SoH(\hat{x})$, which is obtained from the assumed $\hat{x}$. Then, the framework computes the value of x that optimizes NPV based on $SoH(\hat{x})$. The fourth step checks whether the obtained x value is close to $\hat{x}$. If x is very close to $\hat{x}$, x solves the optimization problem with the "correct" SoH of x. Otherwise, the framework updates $\hat{x}$. The updating rule (b1) implies that x is calculated small because $SoH(\hat{x})$ was overestimated. Therefore, it decreases the value of $\hat{x}$ to obtain a lower SoH. The updating rule (b1) treats the opposite case. Figure 5 illustrates the flows of the framework. As with Energy-Fix, the reduced computation can be achieved by using a suboptimal solution to Eq. (13) in the third step. A suboptimal solution in an analytical form can be easily calculated using Eq. (23).

V. SIMULATION RESULTS

We now test the proposed framework using real-world PV generation and market data in South Korea. We use the PV generation data which was measured at every 5 minutes from January 2017 to December 2017 in a PV power station with the capacity of 1,000kW. We consider a forward contract for a PV plus storage system that persists for 15 years. Forward contract prices are given as a combination of the averaged SMP and REC prices in 2017, which are \$83.99/MWh and \$87.11/MWh, respectively. That is, $\lambda_{PV} = \$171.10/\text{MWh}$ and $\lambda_{ESS} = \$(83.99 + \text{Weight} \cdot 87.11)/\text{MWh}$. The capacity of a DC converter should be thoughtfully determined as it limits the maximum instantaneous power from PV generation stored in the ESS. We first set DC converter capacity to 850 kW and then change the capacities in Section V-D. The efficiencies between PV and power grid are set to 95.07%, with 92.24% between the battery and the grid, and 94.05% from solar power to the battery. By adopting the

TABLE 3. Parameter values used for simulations.

Parameter	Value
Contract price for PV generation	171.10($/MWh)
Contract price for ESS discharge	432.43($/MWh) for 4.0 REC
	519.54($/MWh) for 5.0 REC
Efficiency between PV and grid	95.07%
Efficiency between battery and grid	92.24%
Efficiency between PV and battery	94.05%
ESS price without converter	321($/kWh)
Converter price	71($/kW)
Discount rate for NPV	4.5%(per year)
Solar panel degradation	1.0%(per year)

ESS prices of 2018 in [39], we assume a price for ESS excluding the DC converter to be $321/kWh. We assume that the DC converter costs $71/kW,[6] which is a reasonable assumption when considering that the LMO type battery used for battery modeling has a relatively low price. The parameter values used for simulations are summarized in Table 3. In the simulation, DoD is measured from zero SoC. For example, DoD 0.9 is equivalent to a SoC range of 0-0.9. Because it is very difficult to predict the temperature of the batteries in numerical experiments, the temperature of the batteries is assumed to be $25°C$, during all simulations [8], [12], [40]. In practice, the temperature variation of the batteries can be controlled to some extent by means of air-conditioning [8].

A. ESS OPERATION AND BATTERY DEGRADATION

Figure 6 shows the four 24-hour profiles of the PV generation and battery SoC as a result of running the ESS algorithm in Section IV-B when usable capacity is 3,000 kWh and the maximum DoD is 0.75. Charging starts at 10:00 and continues until the maximum SoC level is reached. The battery is discharged at a constant rate from 16:00 to 10:00 the next day until the battery SoC level reaches to zero.

Figure 7 shows an example of SoH curves for Energy-Fix with a usable capacity of 3,500 kWh and DoD-Fix with an initial installation of 3,500 kWh. Figure 7(a) shows that oversizing considerably influences the remaining capacity at the final year in the Energy-Fix case. We observe that with oversizing levels of 10% and 30%, SoH values at year 15 are lower than 0.7 whereas a 50% oversizing level gives more than 0.7. Figure 7(b) shows the SoH curves for different DoD levels. High DoD reduces SoH significantly. If DoD range is 100%, the SoH in the final year is computed as 0.64. Additionally, the gap between the SoH curves become

[6]Because the DC-coupled system is new, there is little information about component prices. $71/kW is a realistic price because the price of the power conversion system of a standalone ESS is expected to be $30/kW in 2018 according to Bloomberg New Energy Finance [39].

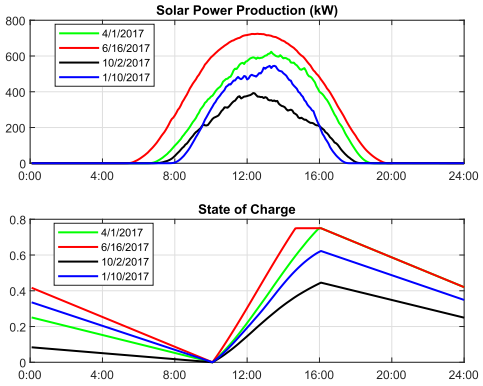

FIGURE 6. Four examples of solar power production and SoC profiles result from the ESS operation algorithm.

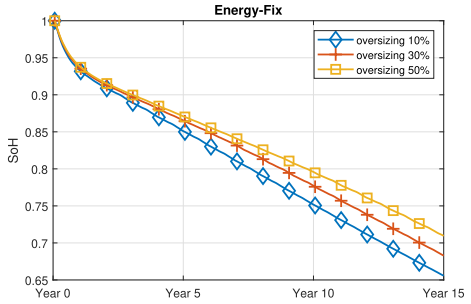

(a) Energy-Fix case with various oversizing levels

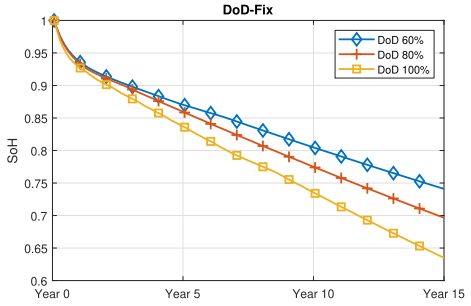

(b) DoD-Fix case with various DoD levels

FIGURE 7. Battery capacity decrease curve of the PV plus ESS system using stress factor coefficients and mathematical modeling in [12].

larger as it approaches the final year. These figures indicate that battery capacity degradation is not a fixed parameter, but rather it is affected by various variables including storage sizes and DoD levels.

It is meaningful to compare SoH curve trends in the two scenarios. All curves decrease steeply during the first years and then gradually decrease. However, as they approach the final year, the SoH curves of Energy-Fix and DoD-Fix show different trends. In the DoD-Fix case, the SoH curves' slopes are relatively constant, which results from a constant DoD range being used for the whole period as depicted in Figure 8(a). In contrast, Energy-Fix uses a constant usable capacity, which results in gradually increasing SoC ranges as shown in Figure 8(b). This explains why the SoH decline accelerated as the curves approach the final year in Figure 7(a).

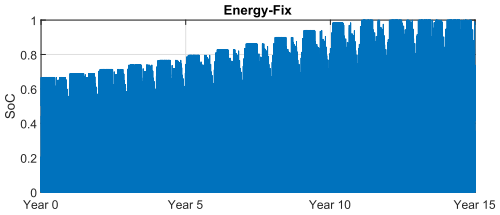

(a) Energy-Fix case

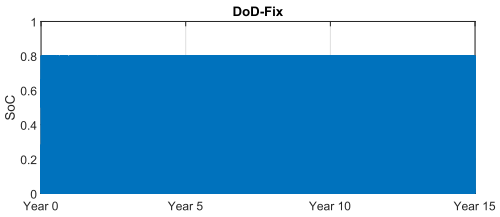

(b) DoD-Fix case when DoD=0.8

FIGURE 8. The SoC for 15 years obtained by applying the ESS operation algorithm.

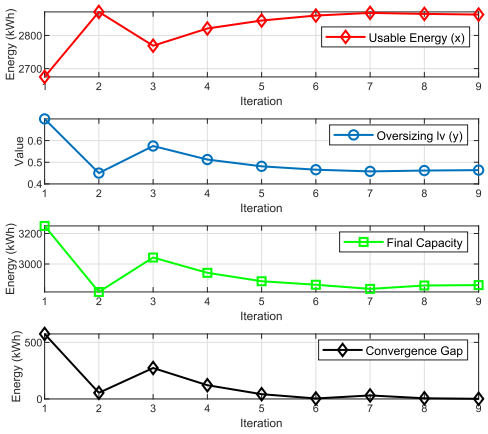

FIGURE 9. ESS capacity, SoH, and convergence gaps calculated at each iteration of the proposed framework for Energy-Fix.

Note that this work employs the mathematical model of battery lifetime in [12] to evaluate battery degradation. Although reference [12] validates the model at $25°C$ for SoH around 80% in the simulation, we consider that the model is still effective for SoH below 80% because the temperature model in [12] is derived from Arrhenius equation which is valid for medium and high temperature condition including $25°C$.

B. CONVERGENCE OF THE ESS SIZING FRAMEWORKS

Figure 9 shows the process of finding the ESS usable capacity, x, and oversizing ratio, y, in the Energy-Fix case. The remaining capacity of the battery at year 15 and the absolute difference between x and $SoH_T(x, y) \cdot (1 + y)x$ are also presented. For the first few iterations, x and y fluctuate and then start to converge after the sixth iteration.

Figure 10 shows x, $\hat{x}$, SoH at year 15, and $|x - \hat{x}|$ values for DoD-Fix. After fluctuating for the first few iterations, x and $\hat{x}$ start to converge after the sixth iteration. The first and third graphs show that the x values from optimization and

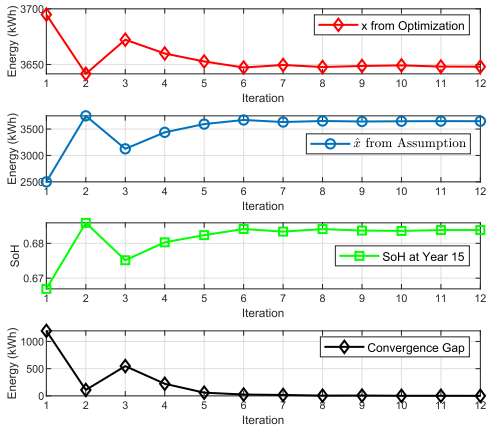

FIGURE 10. ESS capacity, SoH, and convergence gaps calculated at each iteration of the proposed framework for DoD-Fix.

SoH have an inverse relationship. That is, with a high SoH, the framework installs a smaller battery with the expectation that the battery will be degraded gently. In contrast, with a low SoH, the framework installs a larger battery to cope with rapid battery capacity fade.

C. ESS SIZING AND NPV EVALUATION

Table 4 and 5 present ESS sizes, NPV, and benefit-cost ratio (BCR) values obtained from the proposed frameworks for REC weights of 5.0 (adopted by 2019) and 4.0 (scheduled to be implemented in 2020). BCR is the ratio of the sum of discounted revenue throughout the ESS project (or contract period) to ESS installation costs. "Opt." uses Eqs. (9) and (13) to calculate ESS sizes, whereas "Subopt" finds the solution using Eq. (23). Because our focus is to install the ESS to supplement an existing PV system, NPV and BCR are computed based on additional revenues and costs from the ESS installation.

In the Energy-Fix case, the framework gives similar ESS sizes, NPV, and BCR values for each method used to optimize NPV with the same REC weights. However, different REC weights produce significantly different results. The framework requires more capacity when REC weights are high. This is straightforward because a higher REC guarantees greater revenue, which motivates more aggressive investment in the ESS. When the REC weight is 5.0, the ESS installation is highly profitable, showing very high NPV and BCR values. However, with a REC weight of 4.0, the NPV and BCR values will be reduced significantly. When the REC weight changes from 5.0 to 4.0, NPV decreases from \$1,347,429 to \$629,476, which is 53% reduction. Because the forward contract period is 15 years, the NPV of \$629,476 may not be large enough for a power producer to invest in ESS. BCR is also considerably lower when REC weight is 4.0. However, a BCR value greater than 1.5 could be attractive to ESS investors. These results are derived from using the same ESS prices based on 2018 [39] for all case, and declining ESS prices in 2020 will improve the NPV and BCR values presented in Tables 4 and 5. The SoH values in the final year are calculated between 0.67 and

TABLE 4. Calculated ESS sizes and resultant NPV and BCR values in the Energy-Fix case.

REC Weight	Opt. Method	Install. (kWh)	Usable Capacity	Oversizing Ratio	NPV ($)	BCR
5.0	Opt. (9)	4,191	2,863	46.4%	1,347,429	1.96
	Subopt. (23)	4,143	2,827	46.6%	1,345,428	1.97
4.0	Opt. (9)	3,674	2467	48.9%	629,476	1.51
	Subopt. (23)	3,679	2,471	48.9%	629,473	1.51

TABLE 5. Calculated ESS sizes and resultant NPV and BCR values in the DoD-Fix case (DoD=0.9).

REC Weight	Opt. Method	Install. (kWh)	NPV ($)	BCR
5.0	Opt. (13)	3,933	1,452,965	2.10
	Subopt. (23)	3,648	1,438,354	2.17
4.0	Opt. (13)	3,494	737,085	1.62
	Subopt. (23)	3,184	722,694	1.67

0.68 for all cases. We compare the framework with a benchmark to verify its effectiveness. The benchmark calculates the usable capacity as the product of the mean value of α_t, the capacity factor of solar,[7] PV system capacity, and 24 hours, yielding 2, 803 kWh. The oversizing level is thus set to 0.476, the minimum number that satisfies the SoH condition. For a REC weight of 5.0, NPV and BCR values are computed as $1,335,724 and 1.96, respectively. For a REC weight of 4.0, NPV and BCR values are computed as $621,141 and 1.45, respectively. These values are smaller than those obtained by the proposed framework.

Table 5 shows that the solutions are dependent on NPV optimization method in the DoD-Fix case. In DoD-Fix, problem (24) which provides the ESS installation in "Subopt." less accurately approximates the problem that maximizes (21) because $SoH_t(\hat{x})$ is included in β_t and b_t. Like Energy-Fix, NPV is reduced by 49% when REC weight changes from 5.0 to 4.0, and we find that both cases have high BCR values. The values of SoH for the final year are calculated between 0.67 and 0.68. If we consider a benchmark that sets installation capacity to usable capacity in the benchmark in Energy-Fix, NPV and BCR are calculated as $1,261,664 and 2.31, respectively for a REC weight of 5.0. For a REC weight of 4.0, they are obtained as $678,835 and 1.71, respectively. Thus, sizing from the proposed framework produces higher NPV values. If we compare the Energy-Fix and DoD-Fix cases, though comparison would be unfair, DoD-Fix with DoD $= 0.9$ gives higher NPV and BCR values with a similar SoH in the final year than Energy-Fix.

Figure 11 shows ESS installed capacity (kWh) versus PV system capacities (kW) when REC weight is 4.0. The top red curves represent total installed capacity, the middle blue curve shows usable capacity, and the bottom black curve shows

[7]According to the Korean Power Exchange, it was 15.57% in 2017.

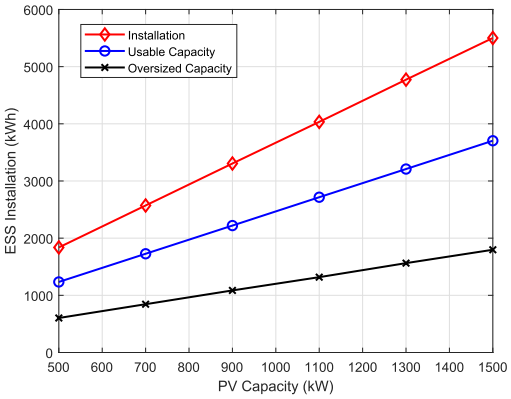

FIGURE 11. ESS capacity (kWh) versus PV system capacity (kW) in the Energy-Fix case. The REC weight is set to 4.0.

oversized kWh added to the usable capacity. The figure shows that there is an almost linear relationship between PV system capacity and ESS installation capacity. Using a curve fitting tool provided in MATLAB R2019a, we found that the linear equation of this curve has a slope of 3.66 and a y-intercept of 6.41, which is almost perfectly fitted to the red curve. This means that the ESS capacity determined by the framework is about 3.66 times that of PV system capacity. The other two curves are almost linear as well. The slope of the middle curve is 2.47, meaning that the usable capacity should be set to 2.47 times that of the PV system's capacity. The oversizing ratio in Figure 11 decreases from 48.95% to 48.52% as PV capacity increases from 500 to 1,500 kW, showing a trivial difference. For a REC weight of 5.0, simulation results show that total ESS installation is 4.19 times that of PV system capacity and usable capacity is 2.86 times that of the PV system capacity. The oversizing ratio decrease from 46.2% to 45.9% as PV capacity increases from 500 to 1,500 kW.

Figure 12 depicts ESS installation versus PV capacity for different REC weights in the DoD-Fix case with DoD $= 0.9$. Both curves are almost linear and have steeper slopes at higher REC weights. For a REC weight 5.0, ESS capacity is 3.93 times of PV capacity whereas it is 3.49 times for a REC weight of 4.0.

From Table 6, DoD levels significantly affects ESS installation and NPV, BCR, and final SoH values. It shows that ESS size becomes smaller as the DoD level increases. This is reasonable as a higher DoD level indicates more efficient battery use. Both NPV and BCR values are significantly improved with increase of DoD. In contrast, the SoH value

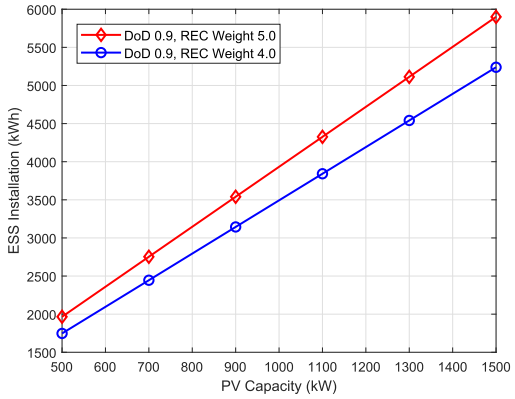

FIGURE 12. ESS capacity (kWh) versus PV system capacity (kW) in the DoD-Fix case.

TABLE 6. ESS sizes, NPV and BCR values, and final SoH in the DoD-Fix case when REC weight is 4.0.

DoD	Install. (kWh)	NPV ($)	BCR	Final SoH
0.7	3,867	47,7413	1.37	0.73
0.8	3,684	622,577	1.50	0.70
0.9	3,494	737,085	1.62	0.67
1.0	3,349	822,912	1.72	0.63

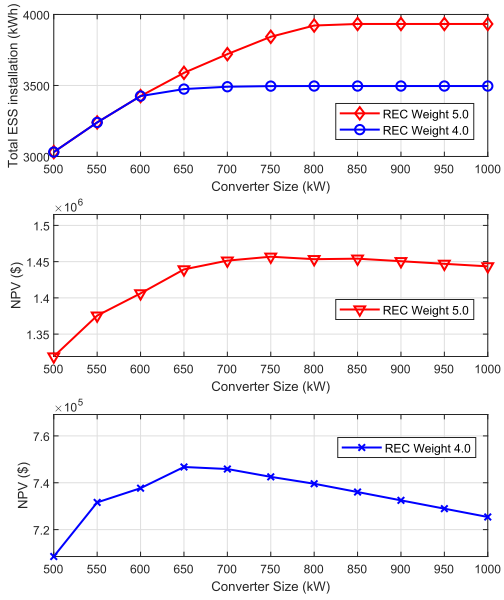

FIGURE 13. ESS capacity (kWh) versus converter size (kW) in the DoD-Fix case.

in the final year decreases as the DoD level grows. If the project owner requires a condition for final SoH, the DoD level should be deliberately selected to satisfy that condition. Otherwise, it is most economically efficient to use a DoD value of 1.0.

D. INFLUENCE OF THE DC CONVERTER

The amount of PV power that can be stored in a battery depends DC converter capacity. Therefore, it is meaningful to analyze the effect of DC converter capacity on ESS installation and resultant NPV value. The topmost panel in Figure 13 shows ESS installation versus converter sizes with different REC weights in the DoD-Fix case. Up to a converter size of 600 kW, ESS installation capacities are equally calculated, irrespective of REC weights. This is not an unexpected finding as a small converter restricts the amount of PV generation that can be stored in a battery. However, with a larger converter, the ESS installation for a REC weight of 5.0 becomes larger than for a REC weight of 4.0. For both REC weights, ESS installation capacities increase with converter sizes and finally saturate when the converter size reaches 850 kW and 800 kW for REC weights 5.0 and 4.0, respectively. From this observation, we notice that installing converters larger than these numbers is not economically efficient. This can be proven by the next two panels in Figure 13, which present the calculation of NPV corresponding to the ESS installation and converter sizes of the topmost panel. We can find that the NPV has the highest value with a converter capacity of 750 kW when the REC weight is 5.0. For a REC weight of 4.0, a converter capacity of 650 kW gives the highest NPV.

VI. CONCLUSION

This study has proposed an advanced ESS sizing framework that considers lithium-ion battery degradation. We have found that battery degradation is affected by ESS operation and sizes, which makes the NPV maximization problem become highly nonlinear and contain black-box parameters. To solve this problem, the proposed framework decomposes the original problem into the evaluation of SoH and optimization of NPV. From a practical point of view, we discussed two scenarios distinguished by how the battery is used over the contract horizon and suggested an ESS sizing framework for each scenario. We calculated ESS sizes, and NPVs and BCR values from the framework with various contract prices, PV capacities, DoD levels, and DC converter sizes. Based on a South Korean type forward contract or PPA, we found that adding ESS to a PV system to make a PV plus storage power plant highly profitable. When REC weight decreases to 4.0 as planned in 2020, NPV and BCR will be reduced considerably. Thus, decreasing ESS costs will be a main issue for maintaining profitability. Additionally, the proposed framework gives improved NPV values, compared to the benchmark cases.

This work allows ESS investors to determine ESS capacity more sophisticatedly than simply treating battery degradation as an independent parameter. Various simulation results conducted in this work can help investors choose ESS size, battery usage methods, DoD levels, and DC converter sizes. This work is based on the South Korean market; however, the proposed framework that interactively assesses SoH and optimizes NPV can be applied to other electricity markets or even to ESS sizing problems in microgrids.

The optimization problem being considered is not guaranteed to be convex and has black-box parameters. Therefore,

we cannot guarantee the optimality of the solutions obtained by the proposed method. Thus, our next step is to develop a more advanced optimization method for solving the problem with black-box parameters. Applying such a method to other applications is our future work.

APPENDIX

A. PROOF OF (9)

To simply express the problem (9), let us define

$$\beta_t \triangleq \gamma^t N \left(\lambda_{ESS} \cdot \rho_{Bat-AC} - \lambda_{PV} \frac{\rho_{PV-AC}}{\rho_{Bat-AC}}\right) \tag{14}$$

$$x' \triangleq Rx \tag{15}$$

$$b_t \triangleq \rho_{PV-Bat} \cdot \alpha_t k^t \tag{16}$$

$$\tilde{w} \triangleq \tilde{G}_{PV} \tag{17}$$

$$c \triangleq C_{ESS}(1+y). \tag{18}$$

Now our objective is to maximize the following function:

$$\begin{aligned}
&\sum_{t=1}^{T} \beta_t \mathbb{E}\left[\min\{x', b_t\tilde{w}\}\right] - \frac{c}{R}x' \\
&= \sum_{t=1}^{T} \beta_t \Big\{ \mathbb{E}\left[\min\{x', b_t\tilde{w}\} | b_t\tilde{w} \le x'\right] \Pr\left[b_t\tilde{w} \le x'\right] \\
&\quad + \mathbb{E}\left[\min\{x', b_t\tilde{w}\} | b_t\tilde{w} > x'\right] \Pr\left[b_t\tilde{w} > x'\right] \Big\} - \frac{c}{R}x'
\end{aligned} \tag{19}$$

with $\Pr[X]$ indicating the probability measure of event X. Eq. (19) can thus be rewritten as

$$\sum_{t=1}^{T} \beta_t \left[\int_{w \le \frac{x'}{b_t}} b_t \tilde{w} f_{\tilde{w}}(w) dw + x' \left(1 - F_{\tilde{w}}\left(\frac{x'}{b_t}\right)\right)\right] - \frac{c}{R}x'$$

where $f_{\tilde{w}}(\cdot)$ is the probability density function of $\tilde{w}$. By taking the first order derivative with respect to x', we can obtain the following optimality condition,

$$\begin{aligned}
&\sum_{t=1}^{T} \beta_t \left[\frac{x'}{b_t} f_{\tilde{w}}\left(\frac{x'}{b_t}\right) + 1 - F_{\tilde{w}}\left(\frac{x'}{b_t}\right) - \frac{x'}{b_t} f_{\tilde{w}}\left(\frac{x'}{b_t}\right)\right] - \frac{c}{R} \\
&\qquad = \sum_{t=1}^{T} \beta_t \left[1 - F_{\tilde{w}}\left(\frac{x'}{b_t}\right)\right] - \frac{c}{R} = 0.
\end{aligned} \tag{20}$$

By plugging Eqs. (14)-(18) to Eq. (20), Eq. (9) can be attained.

B. SUBOPTIMAL SOLUTION TO (9)

If we rewrite (20), we obtain

$$\begin{aligned}
\sum_{t=1}^{T} \beta_t F_{\tilde{w}}\left(\frac{x'}{b_t}\right) &= \sum_{t=1}^{T} \beta_t - \frac{c}{R} \\
&\Rightarrow \sum_{t=1}^{T} \beta_t F_{\tilde{w}}\left(\frac{x'}{b_t}\right) \\
&= \sum_{t=1}^{T} \left(\beta_t - \frac{\beta_t}{\sum_{t=1}^{T}\beta_t} \cdot \frac{c}{R}\right).
\end{aligned} \tag{21}$$

Decomposition of (21) at each t gives us,

$$\beta_t F_{\tilde{w}}\left(\frac{x'_t}{b_t}\right) = \beta_t - \frac{\beta_t}{\sum_{t=1}^{T}\beta_t} \cdot \frac{c}{R} \tag{22}$$

which is a sufficient condition for (21). The solution to (22) is thus calculated as

$$x'_t = b_t F_{\tilde{w}}^{-1}\left(1 - \frac{c}{R\sum_{t=1}^{T}\beta_t}\right).$$

Finally, the suboptimal solution x'_{sub} is obtained as the weighted average of x'_t as:

$$\begin{aligned}
x'_{sub} &= \left(\sum_{t=1}^{T} \frac{x'_t}{b_t}\right) \cdot \left(\sum_{t=1}^{T} \frac{1}{b_t}\right)^{-1} \\
&= T \cdot \left(\sum_{t=1}^{T} \frac{1}{b_t}\right)^{-1} F_{\tilde{w}}^{-1}\left(1 - \frac{c}{R\sum_{t=1}^{T}\beta_t}\right)
\end{aligned} \tag{23}$$

Now we have obtained a suboptimal solution to Eq. (9) in an analytic form by inserting Eqs. (14)-(18) into Eq. (23). It is worth mentioning that x'_{sub} in Eq. (23) is the solution to the problem, instead of maximizing (19):

$$\max_{x'} \mathbb{E}\left[\left(\sum_{t=1}^{T}\beta_t\right) \min\left\{x', T\left(\sum_{t=1}^{T}\frac{1}{b_t}\right)^{-1} \cdot \tilde{w}\right\}\right] - \frac{c}{R}x'. \tag{24}$$

REFERENCES

[1] (2018). *Lazard's Levelized Cost of Storage Analysis—Version 4.0*. Accessed: Mar. 15, 2020. [Online]. Available: https://www.lazard.com/media/450774/lazards-levelized-cost-of-storage-version-40-vfinal.pdf

[2] B. Dunn, H. Kamath, and J.-M. Tarascon, "Electrical energy storage for the grid: A battery of choices," *Science*, vol. 334, no. 6058, pp. 928–935, Nov. 2011.

[3] L. Lu, X. Han, J. Li, J. Hua, and M. Ouyang, "A review on the key issues for lithium-ion battery management in electric vehicles," *J. Power Sour.*, vol. 226, pp. 272–288, Mar. 2013.

[4] G. Ning and B. N. Popov, "Cycle life modeling of lithium-ion batteries," *J. Electrochemical Soc.*, vol. 151, no. 10, pp. A1584–A1591, 2004.

[5] R. Spotnitz, "Simulation of capacity fade in lithium-ion batteries," *J. Power Sour.*, vol. 113, no. 1, pp. 72–80, Jan. 2003.

[6] J. Vetter *et el.*, "Ageing mechanisms in lithium-ion batteries," *J. Power Sour.*, vol. 147, nos. 1–2, pp. 269–281, 2005.

[7] O. Erdinc, B. Vural, and M. Uzunoglu, "A dynamic lithium-ion battery model considering the effects of temperature and capacity fading," in *Proc. Int. Conf. Clean Electr. Power*, Jun. 2009, pp. 383–386.

[8] D.-I. Stroe, M. Swierczynski, A.-I. Stroe, R. Laerke, P. C. Kjaer, and R. Teodorescu, "Degradation behavior of lithium-ion batteries based on lifetime models and field measured frequency regulation mission profile," *IEEE Trans. Ind. Appl.*, vol. 52, no. 6, pp. 5009–5018, Nov. 2016.

[9] D.-I. Stroe, V. Knap, M. Swierczynski, A.-I. Stroe, and R. Teodorescu, "Operation of a grid-connected lithium-ion battery energy storage system for primary frequency regulation: A battery lifetime perspective," *IEEE Trans. Ind. Appl.*, vol. 53, no. 1, pp. 430–438, Jan. 2017.

[10] X. Hu, H. Yuan, C. Zou, Z. Li, and L. Zhang, "Co-estimation of state of charge and state of health for lithium-ion batteries based on fractional-order calculus," *IEEE Trans. Veh. Technol.*, vol. 67, no. 11, pp. 10319–10329, Nov. 2018.

[11] X. Hu, F. Feng, K. Liu, L. Zhang, J. Xie, and B. Liu, "State estimation for advanced battery management: Key challenges and future trends," *Renew. Sustain. Energy Rev.*, vol. 114, Oct. 2019, Art. no. 109334.

[12] B. Xu, A. Oudalov, A. Ulbig, G. Andersson, and D. S. Kirschen, "Modeling of lithium-ion battery degradation for cell life assessment," *IEEE Trans. Smart Grid*, vol. 9, no. 2, pp. 1131–1140, Mar. 2018.

[13] J. Mitra, "Reliability-based sizing of backup storage," *IEEE Trans. Power Syst.*, vol. 25, no. 2, pp. 1198–1199, May 2010.
[14] R. Fernandez-Blanco, Y. Dvorkin, B. Xu, Y. Wang, and D. S. Kirschen, "Optimal energy storage siting and sizing: A WECC case study," *IEEE Trans. Sustain. Energy*, vol. 8, no. 2, pp. 733–743, Apr. 2017.
[15] S. Wogrin and D. F. Gayme, "Optimizing storage siting, sizing, and technology portfolios in transmission-constrained networks," *IEEE Trans. Power Syst.*, vol. 30, no. 6, pp. 3304–3313, Nov. 2015.
[16] H. Oh, "Optimal planning to include storage devices in power systems," *IEEE Trans. Power Syst.*, vol. 26, no. 3, pp. 1118–1128, Aug. 2011.
[17] S. Bahramirad, W. Reder, and A. Khodaei, "Reliability-constrained optimal sizing of energy storage system in a microgrid," *IEEE Trans. Smart Grid*, vol. 3, no. 4, pp. 2056–2062, Dec. 2012.
[18] F. Zhang, Y. Song, and Z. Hu, "Mixed-integer linear model for transmission expansion planning with line losses and energy storage systems," *IET Gener., Transmiss. Distrib.*, vol. 7, no. 8, pp. 919–928, Aug. 2013.
[19] T. Qiu, B. Xu, Y. Wang, Y. Dvorkin, and D. S. Kirschen, "Stochastic multistage coplanning of transmission expansion and energy storage," *IEEE Trans. Power Syst.*, vol. 32, no. 1, pp. 643–651, Jan. 2017.
[20] S. Dehghan and N. Amjady, "Robust transmission and energy storage expansion planning in wind farm-integrated power systems considering transmission switching," *IEEE Trans. Sustain. Energy*, vol. 7, no. 2, pp. 765–774, Apr. 2016.
[21] P. Harsha and M. Dahleh, "Optimal sizing of energy storage for efficient integration of renewable energy," in *Proc. IEEE Conf. Decis. Control Eur. Control Conf.*, Dec. 2011, pp. 5813–5819.
[22] A. Arabali, M. Ghofrani, M. Etezadi-Amoli, and M. S. Fadali, "Stochastic performance assessment and sizing for a hybrid power system of Solar/Wind/Energy storage," *IEEE Trans. Sustain. Energy*, vol. 5, no. 2, pp. 363–371, Apr. 2014.
[23] T. K. A. Brekken, A. Yokochi, A. von Jouanne, Z. Z. Yen, H. M. Hapke, and D. A. Halamay, "Optimal energy storage sizing and control for wind power applications," *IEEE Trans. Sustain. Energy*, vol. 2, no. 1, pp. 69–77, Jan. 2011.
[24] E. Nasrolahpour, S. J. Kazempour, H. Zareipour, and W. D. Rosehart, "Strategic sizing of energy storage facilities in electricity markets," *IEEE Trans. Sustain. Energy*, vol. 7, no. 4, pp. 1462–1472, Oct. 2016.
[25] P. Harsha and M. Dahleh, "Optimal management and sizing of energy storage under dynamic pricing for the efficient integration of renewable energy," *IEEE Trans. Power Syst.*, vol. 30, no. 3, pp. 1164–1181, May 2015.
[26] R. Arghandeh, J. Woyak, A. Onen, J. Jung, and R. P. Broadwater, "Economic optimal operation of community energy storage systems in competitive energy markets," *Appl. Energy*, vol. 135, pp. 71–80, Dec. 2014.
[27] K. Bradbury, L. Pratson, and D. Patiño-Echeverri, "Economic viability of energy storage systems based on price arbitrage potential in real-time U.S. electricity markets," *Appl. Energy*, vol. 114, pp. 512–519, Feb. 2014.
[28] Y. J. Zhang, C. Zhao, W. Tang, and S. H. Low, "Profit-maximizing planning and control of battery energy storage systems for primary frequency control," *IEEE Trans. Smart Grid*, vol. 9, no. 2, pp. 712–723, Mar. 2018.
[29] H. T. Le and T. Q. Nguyen, "Sizing energy storage systems for wind power firming: An analytical approach and a cost-benefit analysis," in *Proc. IEEE Power Energy Soc. Gen. Meeting-Convers. Del. Elect. Energy 21st Century*, Jul. 2008, pp. 1–8.
[30] M. Dicorato, G. Forte, M. Pisani, and M. Trovato, "Planning and operating combined wind-storage system in electricity market," *IEEE Trans. Sustain. Energy*, vol. 3, no. 2, pp. 209–217, Apr. 2012.
[31] R. Fu, T. W. Remo, and R. M. Margolis, "2018 US utility-scale photovoltaics-plus-energy storage system costs benchmark," Nat. Renew. Energy Lab., Golden, CO, USA, Tech. Rep., 2018.
[32] N. A. DiOrio, J. M. Freeman, and N. Blair, "DC-connected solar plus storage modeling and analysis for Behind-The-Meter systems in the system advisor model," in *Proc. IEEE 7th World Conf. Photovoltaic Energy Convers. (WCPEC) (Joint Conf. 45th IEEE PVSC, 28th PVSEC 34th EU PVSEC)*, Jun. 2018, pp. 3777–3782.
[33] G. Media. *Dc-Coupled Solar-Plus-Storage Systems are Gaining Ground*. Accessed: Mar. 15, 2020. [Online]. Available: https://www.greentechmedia.com/articles/read/dc-coupled-solar-plus-storage-gaining-ground#gs.w8fzr1
[34] H. Shin and R. Baldick, "Mitigating market risk for wind power providers via financial risk exchange," *Energy Econ.*, vol. 71, pp. 344–358, Mar. 2018.
[35] H. Shin, D. Lee, and R. Baldick, "An offer strategy for wind power producers that considers the correlation between wind power and real-time electricity prices," *IEEE Trans. Sustain. Energy*, vol. 9, no. 2, pp. 695–706, Apr. 2018.
[36] M. Vilim and A. Botterud, "Wind power bidding in electricity markets with high wind penetration," *Appl. Energy*, vol. 118, pp. 141–155, Apr. 2014.
[37] S. Downing and D. Socie, "Simple rainflow counting algorithms," *Int. J. Fatigue*, vol. 4, no. 1, pp. 31–40, Jan. 1982.
[38] E. Peled, "The electrochemical behavior of alkali and alkaline earth metals in nonaqueous battery systems—The solid electrolyte interphase model," *J. Electrochem. Soc.*, vol. 126, no. 12, pp. 2047–2051, 1979.
[39] "Energy storage system costs survey 2018," Bloomberg New Energy Finance, New York, NY, USA, Tech. Rep., 2018.
[40] M. Wierczy Ski, D. I. Stroe, R. Laerke, A. I. Stan, P. C. Kjaer, R. Teodorescu, and S. K. Kaer, "Field experience from li-ion BESS delivering primary frequency regulation in the Danish energy market," *ECS Trans.*, vol. 61, no. 37, pp. 1–14, Sep. 2014.

HUNYOUNG SHIN (Member, IEEE) received the B.S. degree in radio and communication engineering and the M.S. degree in electrical engineering from Korea University, Seoul, South Korea, and the Ph.D. degree from the Electrical and Computer Engineering Department, The University of Texas at Austin, Austin, TX, USA, in December 2017. In 2018, he joined LG CNS as a Managing Consultant and has participated in energy storage system planning projects. He is currently an Assistant Professor at Sangmyung University, Seoul. His research interests are primarily in optimization of power systems, risk-hedging strategies, and pricing rule in electricity markets.

JAE HYUNG ROH (Member, IEEE) received the B.S. degree in nuclear engineering from Seoul National University, Seoul, South Korea, in 1993, the M.S. degree in electrical engineering from Hongik University, South Korea, in 2002, and the Ph.D. degree in electrical engineering from the Illinois Institute of Technology, Chicago, IL, USA. From 1992 to 2001, he was with Korea Electric Power Corporation. From 2001 to 2010, he was with Korea Power Exchange. Since 2010, he has been with the Electrical Engineering Department, Konkuk University, Seoul, where he is currently an Associate Professor. His research interests include power systems restructuring, smart grid, and resource planning.